Journal of Power Sources 185 (2008) 670–675

Contents lists available at ScienceDirect

Journal of Power Sources

journal homepage: www.elsevier.com/locate/jpowsour

Synthesis and characterization of $LaNiO_3$-based platinum catalyst for methanol oxidation

A. Balasubramanian, N. Karthikeyan, V.V. Giridhar*

Electrodics and Electrocatalysis Division, Central Electrochemical Research Institute, Karaikudi 630006, Tamilnadu, India

ARTICLE INFO

Article history:
Received 9 May 2008
Received in revised form 15 July 2008
Accepted 21 August 2008
Available online 9 September 2008

Keywords:
Perovskite
Lanthanum nickelate
Precursor complex route
Methanol electro-oxidation
Fuel cell

ABSTRACT

Conductive perovskite type lanthanum nickelate ($LaNiO_3$) powders are prepared through a nitrilotriacetic acid (NTA) precursor complex route. Differential thermal analysis (DTA) and thermogravimetric analysis (TGA) results indicate complete decomposition of the precursor complex to $LaNiO_3$ at 900 °C in 4 h. Powder X-ray diffraction (XRD) patterns confirm the formation of the perovskite. Scanning electron microscopic (SEM) analysis and particle size determination reveal the formation of micron-sized particles, probably by the agglomeration of nanoparticles of $LaNiO_3$. Cyclic voltammetry (CV) is used to assess the electrochemical activity of $LaNiO_3$ in comparison with Pt/C, as well as the addition of small amounts of Pt/C to $LaNiO_3$ or a Vulcan XC-72R carbon support of three different compositions, towards methanol electro-oxidation. $LaNiO_3$ does not show much activity for methanol oxidation. However, a synergistic effect is observed when $LaNiO_3$ is mixed with small amounts of Pt/C. The increased oxidation current due to the addition of $LaNiO_3$ to small amounts of Pt/C in the three mixtures containing $LaNiO_3$ is attributed to either the additional catalyst site of the perovskite in addition to the Pt site, or the removal of CO poisoning on the Pt surface by the surface oxygen of the adjacent perovskite.

1. Introduction

One of the technical restrictions currently inhibiting the development of direct methanol fuel cells (DMFCs) is the poisoning of the anode catalyst by the CO intermediate. Platinum-based catalysts are the most efficient materials for methanol oxidation [1]. Despite the great deal of effort devoted to the search for new catalysts, Pt–Ru alloy is still the most active anode material for methanol oxidation [2]. The methanol oxidation proceeds by the well-known bifunctional mechanism on Pt–Ru alloy, in which Pt is the main catalyst favouring the adsorption of methanol (performing the tasks of bond-breaking in H–H, O–H and C–H groups) and the oxophilic Ru adjacent to Pt removes the intermediate CO [3].

Since mixed metal oxides based on perovskites of ABO_3 structure (where A and B are cations) are oxygen-containing species with good proton transport properties, electronically conductive, their surfaces being acidic and hence expected to be active and stable in acidic environment [4], it was felt that substitution of Ru by perovskite electrocatalysts in the Pt–Ru bimetallic system may improve the catalysis of methanol oxidation. Some of the above-mentioned properties of perovskites can be varied by choosing different combinations of A and B cations, where A is a larger cation and B is a small transition metal cation [5]. Additional variation can be effected by choosing appropriate A and B cations in order to obtain perovskites of the form $A^{3+}B^{3+}O_3$, $A^{2+}B^{4+}O_3$, $A^{+}B^{5+}O_3$, or by partial substitution of either A ion with another A′ ion to give $A_{1-x}A'_xBO_3$, or B ion with B′ ion to give $AB_{1-x}B'_xO_3$.

Perovskites have been used as anode catalyst for methanol oxidation in two ways. In the first category, perovskite catalysts without Pt or Ru in either of the A or B sites were evaluated for electrochemical oxidation of methanol and a comparison was made with either Pt/C or standard Pt–Ru/C. In the second category perovskite catalysts with either Pt or Ru present in the B site of perovskite structure itself were examined for methanol oxidation and a comparison was made again with state-of-the-art Pt–Ru/C catalysts. In the former category, the work of Zhou et al. [6] can be cited—wherein a series of rare-earth perovskite powders, namely, $La_{1-x}Mn_{1-y}O_{3-\delta}$, $La_{1-x}Fe_{1-y}O_{3-\delta}$, $La_{1-x}Cr_{1-y}O_{3-\delta}$, $La_{1-x}Ni_{1-y}O_{3-\delta}$, $(La, Sr)_{1-x}Fe_{1-y}O_{3-\delta}$, $La_{1-x}(Fe, Ca)_{1-y}O_{3-\delta}$ ($0.0 < x$, $y < 0.2$) were used to study methanol oxidation. Among these perovskites, $La_{1-x}Fe_{1-y}O_{3-\delta}$ and $La_{1-x}Mn_{1-y}O_{3-\delta}$ were found to be stable in aqueous methanol solutions and the former gave reasonably good electrocatalytic activity for methanol oxidation in comparison with Pt/C and Pt–Ru/C electrocatalysts in addition to showing a lower on-set potential. In the second category, White and Sammells [7] studied a large number of per-

* Corresponding author. Tel.: +91 4565 227550–559x404; fax: +91 4565 227713.
E-mail address: gvadari@yahoo.com (V.V. Giridhar).

0378-7753/$ – see front matter © 2008 Elsevier B.V. All rights reserved.
doi:10.1016/j.jpowsour.2008.08.096

ovskites containing Sm, Ce, Sr, Pb, La, Ba, Nd in the A site and Co, Pt, Pd, Ru in the B site for methanol oxidation. They found good electrochemical activity for the following perovskite compounds: $SrRu_{0.5}Pt_{0.5}O_3$, $SrRu_{0.5}Pd_{0.5}O_3$, $SrPdO_3$, $SmCoO_3$, $SrRuO_3$, $La_{0.8}Ce_{0.2}CoO_3$, $SrTi_{0.5}Co_{0.5}O_3$ and $La_{0.8}Sr_{0.2}CoO_3$. Among these, the best one, viz., $SrRu_{0.5}Pt_{0.5}O_3$, gave a methanol oxidation current density of 28 mA cm^{-2} at 0.45 V vs. SCE. An attempt was also made to correlate the maximum power densities of their DMFC systems containing the perovskite anode catalysts with solid state and thermodynamic parameters such as lattice molecular polarizability (α), optical dielectric constant (ε), lattice free volume (V_f), perovskite spin only magnetic moment (I_s), the number of d-electrons in perovskite A and B lattice sites (n_d), the average metal–oxygen binding energy for the perovskite lattice (E_{M-O}), and the lattice constant (α_o^n). The relative importance of these parameters in making such a correlation was determined. It was found that methanol oxidation electrocatalysis was primarily influenced by the optical dielectric constant ε and molecular electronic polarizability α. Another work in the second category mentioned above was that of Lan et al. [4], who studied perovskite electrocatalysts in which B site contained Ru. The compounds included $SrRuO_3$, $LaRuO_3$, $BaRuO_3$, $CaRuO_3$, $SrFeO_3$ and complex perovskite–Pt catalysts where Pt was introduced during the formation of the perovskite structure itself. In fact, the last compound containing both Pt and perovskite was used because even though Ru was present in the B site of the perovskite structure and such systems are promising candidates for the development of effective catalysts; the performance was not comparable with that of state-of-the-art Pt–Ru/C. Nevertheless, an optimum complex perovskite–Pt catalyst composition ($LaRuO_3$ + 15 wt% Pt) was determined, i.e., one that could deliver superior performance compared with standard Pt–Ru in real fuel cell systems. The stability of the catalyst was also tested by chronoamperometry and found to be stable up to 1 h without showing any deterioration.

We followed a different approach in which only Ru was replaced, and not Pt, in the Pt–Ru system by the perovskite and study its effect on methanol oxidation. Although a microstructure containing Pt flanked by a perovskite compound on either side is difficult to synthesize in order to achieve the bifunctional behaviour discussed as above, it has been attempted to study the effect of addition of perovskite to Pt/C on methanol oxidation by physically mixing these two powders. Further, to our knowledge, there are no reports of the use of $LaNiO_3$ as an anode catalyst for methanol oxidation.

Generally, perovskite type oxides are prepared by (i) high-energy ball milling directly from the oxide precursors followed by combustion [8]; (ii) decomposition of precursor complexes based on citrate, ethylenediamminetetraacetate (EDTA), diethylenetriaminepenta acetate (DTPA) ligands [9–11]; (iii) aqueous combustion synthesis using glycine as the fuel and respective metal nitrates of the perovskite components as oxidizers [12]. In the present work, we have adopted the method of decomposition of a precursor complex based on nitrilotriacetic acid (NTA) to prepare $LaNiO_3$. These powders were then used either alone or mixed with Pt/C of different ratios for studying their electrochemical behaviour towards methanol oxidation.

2. Experimental

2.1. Synthesis of $LaNiO_3$

The synthesis of $LaNiO_3$ was carried out according to the procedure of Wang et al. [11]. This involved decomposition of a precursor complex that used La $(NO_3)_3{\cdot}6H_2O$, Ni$(NO_3)_2{\cdot}6H_2O$ and NaOH as starting materials and NTA as the complexing agent.

2.2. Preparation of Pt/C

The Pt/C was prepared by the colloidal precipitation route of Ravi kumar and Shukla [13] which employed a precursor complex $Na_6Pt(SO_3)_4$. This complex was prepared by taking chloroplatinic acid solution (1 g 100 ml^{-1}) and adjusting the pH to 7 by adding Na_2CO_3 solution. The solution pH was then lowered to an acidic range (preferably near 3) by adding $NaHSO_3$ solution. The solution was gently warmed until it became colourless. The pH of the solution was then raised to 6 by adding Na_2CO_3 solution, when a white precipitate of $Na_6Pt(SO_3)_4$ was obtained. The precipitate was filtered over a 0.45 μ membrane filter paper, washed copiously with milli-Q water to remove chloride ions, and then dried in an air oven at 80 °C for 2 h. A precursor complex solution of required concentration was taken and diluted to 750 ml with double-distilled water in a 2 l beaker having a magnetic pellet for continuous stirring. To this solution, 100 ml of H_2O_2 (30%) from a burette was added drop by drop. During the addition, the temperature of the Pt precursor complex solution was maintained at 80 °C. It took nearly 90 min to complete the addition of reagents. At the end of these additions, colloidal particles of Pt oxides were formed.

The required amount of Vulcan XC-72R was dispersed in milli-Q water and heated to 80 °C for about 30 min. It was then sonicated for about 30 min until a good slurry was formed. The slurry was then added to the colloidal Pt oxide solution, taking care to maintain the temperature of the solution at 80 °C. After 30 min of equilibration, Iolar grade hydrogen was passed through this solution for about 60 min to give rise to vigorous bubbling. The temperature was maintained at 80 °C during this period. At the end, the reduction of Pt oxides to Pt occurred and Pt particles supported on carbon were formed. The solution was then filtered over a 0.45-μ Millipore membrane filter paper and the solid powder was dried in an air oven at 80 °C for about 2 h. The catalyst particles so obtained on Vulcan XC-72R are black powders. The synthesized Pt/C was mixed either with $LaNiO_3$ or with carbon (Vulcan XC-72R) in various ratios and ground together. The resulting mixture was coated on a glassy carbon (GC) substrate to evaluate its electrochemical characteristics towards methanol oxidation.

2.3. Physico-chemical characterization

TGA and DTA analyses of the precursor complexes were carried out using a SDT Q600 (TA Instruments) thermal analyzer with a heating rate of 10 °C per minute and under atmospheric conditions. XRD characterization of $LaNiO_3$ was carried out with an X'Pert PRO system (powder XRD, PANalytical model PW 3040/60) using a Cu Kα line at 0.1540 nm. The step size of the 2θ scans was 0.05°. Particle-size distribution analysis was carried out in a (HORIBA LA-910) laser scattering analyzer that was capable of measuring average particle sizes in the range of 0.02–1020 μm. SEM photographs were taken in order to examine the particle morphology of the perovskite by using a JEOL scanning electron microscope (model JSM35CF) operating at an accelerating voltage of 25 kV. Electrical conductivity of the perovskite material was measured in air at room temperature using a d.c. four-probe method with a combination of a Keithley 2400 digital source meter and a Keithley 2182 Nanovoltmeter.

2.4. Electrochemical characterization

The electrochemical characterization of the catalysts was undertaken by using a computer-controlled model 273 A EG&G PAR electrochemical system using a three-electrode setup. Cyclic voltammograms (CVs) of the different powders (viz., $LaNiO_3$, various compositions of Pt/C mixed with $LaNiO_3$ and Pt/C) coated on

glassy carbon (GC) electrode (working electrode) were recorded to determine the activity towards methanol oxidation. A Hg/Hg_2SO_4, 0.05 M H_2SO_4 (MMS) reference electrode and a 1 cm × 1 cm Pt foil counter electrode were employed. A 1.0 M solution of methanol (SRL) prepared in 0.5 M H_2SO_4 served as the electrolyte. A glass cell that had provision for the introduction of the three electrodes and the bubbling of nitrogen was employed in the present study. The contents of the cell were stirred with a magnetic stirrer. All the experiments were performed at room temperature, which was close to 30 °C.

2.4.1. Cyclic voltammetric studies

The evaluation of intrinsic electrocatalytic activity of Pt supported on high surface area carbon or $LaNiO_3$-mixed Pt/C or carbon-mixed Pt/C was done by coating the catalyst on a GC substrate (2.4 mm dia.) as a thin film. Prior to that, the GC was polished to a mirror finish by using alumina slurry on 5/0 and 6/0 emery papers (Premier, Kohinoor Products, India) for about 30 min. A 10 μl aliquot of an aqueous suspension of the catalyst (3.5 mg of the catalyst sonicated in 1 μl 5 wt% Nafion solution in aliphatic alcohols, 2.0 ml of Milli-Q water and 2 ml isopropanol) was pipetted on the GC and dried under a 60 W tungsten filament lamp.

3. Result and discussion

3.1. Analysis of thermal decomposition of precursor complex

Fig. 1 shows the TGA and DTA curves for the decomposition of precursor complex. The weight loss region from 40 to 145 °C of the TGA curve can be attributed to the loss of coordinated water. The region between 200 and 325 °C may be attributed to the loss of some organic groups including methylamino and hydrocarbon groups. The region between 325 and 395 °C may be due to the cleavage of bonds between the metal and the carboxyl groups of the precursor. The region between 395 °C and up to 491 °C is attributed to the formation of oxides of La and Ni. The region beyond 491 °C may be attributed to the rearrangement of these oxides to the perovskite $LaNiO_3$ as there are minimum weight losses in these regions.

In the DTA curve, two small exothermic humps and a sharp and strong exothermic peak occur in the regions 297–365 °C, 420–520 °C and 391 °C (peak value), respectively. These regions and the peak value can be matched with processes such as the decomposition of organic groups, the formation of oxides and the cleavage of bonds between metal and carboxyl groups of the precursor, respectively. The DTA curve also shows no sharp change

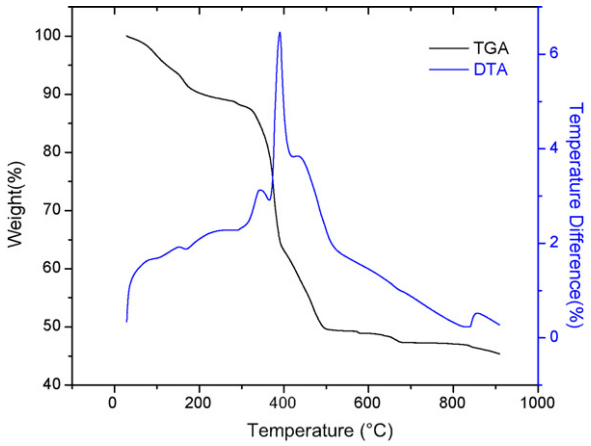

Fig. 1. TGA and DTA for La, Ni and NTA based precursor complex.

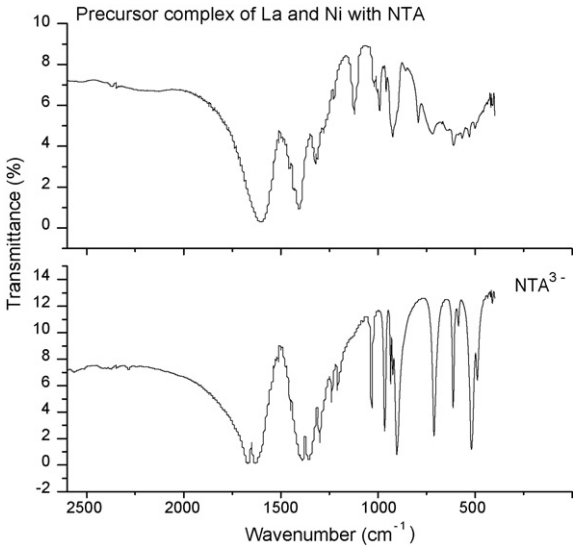

Fig. 2. FT-IR spectra of NTA^{3-} and NTA complexes of La and Ni.

in temperature beyond 520 °C and this can be attributed to the formation of $LaNiO_3$ from the individual oxides of La and Ni.

3.2. FT-IR characterization of precursor complexes of NTA with La and Ni

FT-IR spectra of NTA^{3-} and the precursor complex of La and Ni are shown in Fig. 2. The FT-IR spectra of NTA^{3-} shows a band around 1630–1670 cm^{-1} that can be assigned to the asymmetric vibrations of the deprotonated carboxylic acid group, while the peak close to 1356–1391 cm^{-1} is due to the corresponding symmetric stretching mode. The signals in the region from 965 to 1239 cm^{-1} can be assigned to CN and CC stretching modes. The complexes formed by La and Ni with NTA show bands of weak intensity at frequencies similar to that of NTA^{3-}, but they correspond to broadening of bands. The broadening of the band in the region corresponding to deprotonated carboxylic acid and C–N group indicates that the oxygen and nitrogens of the respective groups participate in the complex formation with the metal ions.

3.3. Analysis of formation of $LaNiO_3$ crystal structure

The XRD pattern of the calcinated catalyst powder (900 °C, 4 h) is shown in Fig. 3 and indicates that the material is crystalline. The d-spacing values of calcinated catalyst powder match well with the standard XRD pattern of $LaNiO_3$ (JCPDS file no. 010-792448) and hence confirmed the formation of $LaNiO_3$. This belongs to a

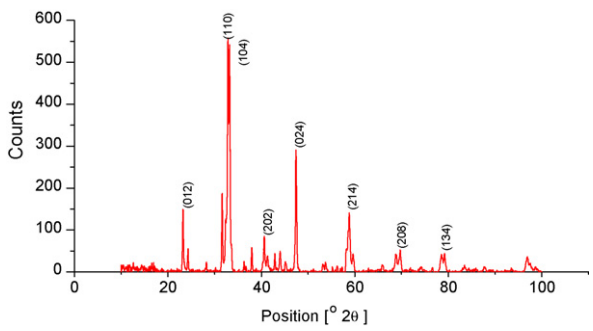

Fig. 3. XRD patterns of calcinated catalyst powder at 900 °C for 4 h for formation of $LaNiO_3$.

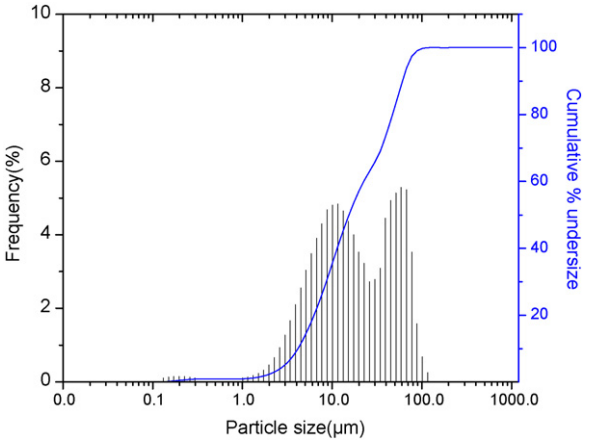

Fig. 4. Particle-size distribution of $LaNiO_3$ powder.

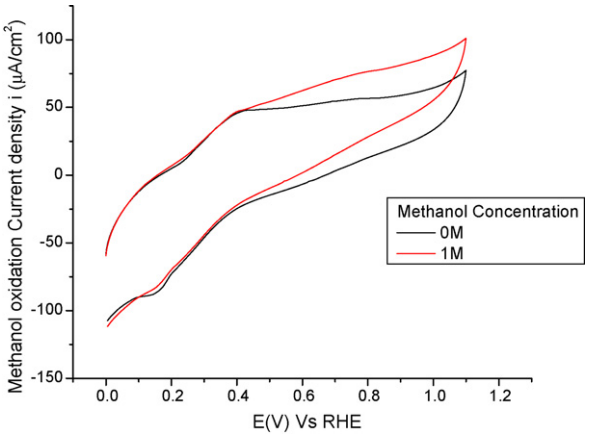

Fig. 6. Cyclic voltammograms for methanol oxidation at $LaNiO_3$ coated over glassy carbon electrode in 0.5 M H_2SO_4.

rhombohedral crystal system with an *R*-3*C* space group. The lattice parameters obtained for this compound in the present work are $a = b = 5.4563$ Å, $c = 13.1276$ Å [14], which is comparable with the same standard XRD pattern $a = b = 5.4535$ Å; $c = 13.1010$ Å. The average particle size (D) was calculated from the Scherrer equation, $D = K\lambda/\beta\cos\theta$, where D is the average crystal size, K is the Scherrer constant equal to 0.89, λ is the X-ray wavelength equal to 0.1542 nm, β is the full width at half-maximum (FWHM), and θ is the diffraction angle. The value is found to be ≈64 nm. The electrical conductivity for $LaNiO_3$ is lower than that reported by Wang et al. [11] and was 6.125×10^{-2} S cm^{-1} at room temperature.

3.4. Particle-size distribution and surface morphology of $LaNiO_3$

Particle size analysis of the synthesized $LaNiO_3$ powders reveals a wide range of particle sizes (Fig. 4); the smaller particles join together for form larger particles. This is corroborated by SEM images (Fig. 5) which show the presence of small as well as large-sized flake-like particles. It appears that the growth of the particles is preferentially in one direction. There are no sharp edges in any of the particles and this could be due to agglomeration of much smaller sized particles. Determination of particle size by the laser scattering method was used to arrive at the mean aggregate diameter of the $LaNiO_3$ catalyst particles, which is found to be 25.37 μm with a most probable diameter of 10 μm.

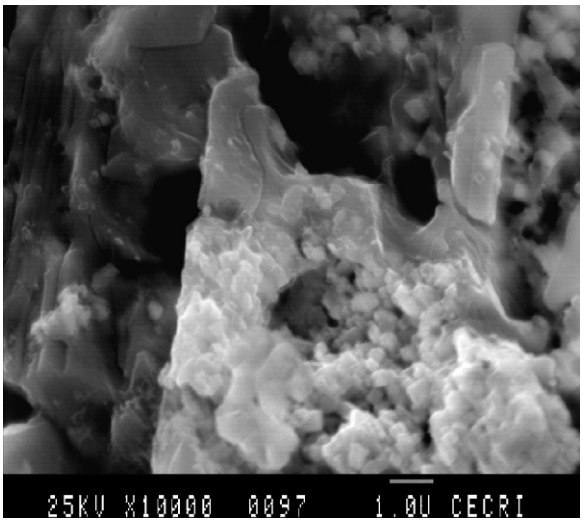

Fig. 5. Scanning electron micrographs of $LaNiO_3$ powder.

3.5. Electrochemical characterization

The evaluation of the intrinsic electrocatalytic activity of $LaNiO_3$-based catalysts with and without platinized carbon mixing is usually undertaken by coating the catalyst on a GC surface in the form of a thin film and then performing CVs, as described earlier. After cleaning of the GC electrode, a 1 μl aliquot of aqueous suspension of the catalyst (which was earlier obtained by ultrasonically dispersing 3.5 mg of the catalyst in 0.5 ml of pure water) was suspended on the GC surface by using a micropipette. The catalyst-coated GC electrode was kept under a 60 W-tungsten filament lamp and dried. After ensuring that the catalyst has covered the GC surface (by noting the non-shiny appearance of the GC surface), 5 μl of a diluted solution of 5% Nafion 117 was placed on top of the dried catalyst powder and further dried under the lamp to form a thin coating. The film thickness was adjusted in such a way that there were no mass transport limitations across the film.

Cyclic voltammograms of $LaNiO_3$ and Pt/C were performed in 0.5 M H_2SO_4 in the absence and presence of methanol (final concentration = 1 M) and are shown in Figs. 6 and 7, respectively. The CV for methanol oxidation on $LaNiO_3$ indicates that there is only

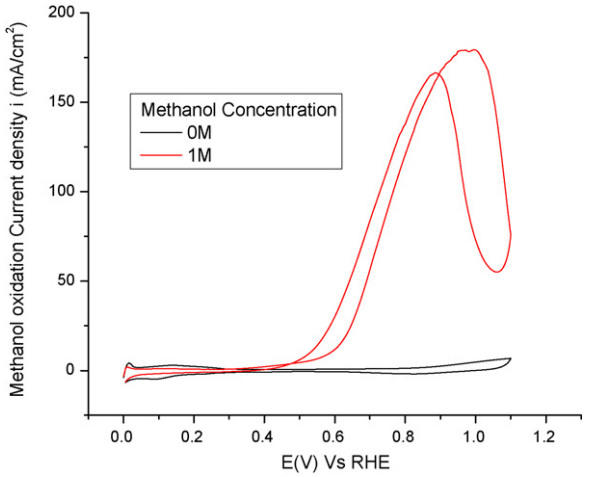

Fig. 7. Cyclic voltammograms for methanol oxidation at Pt/C coated over glassy carbon electrode in 0.5 M H_2SO_4.

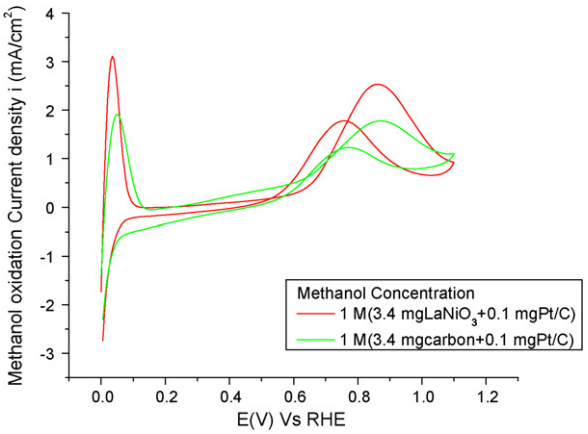

Fig. 8. Cyclic voltammograms for methanol oxidation at 3.4 mg $LaNiO_3$ + 0.1 mg Pt/C and 3.4 mg carbon + 0.1 mg Pt/C coated over glassy carbon electrode in 0.5 M H_2SO_4.

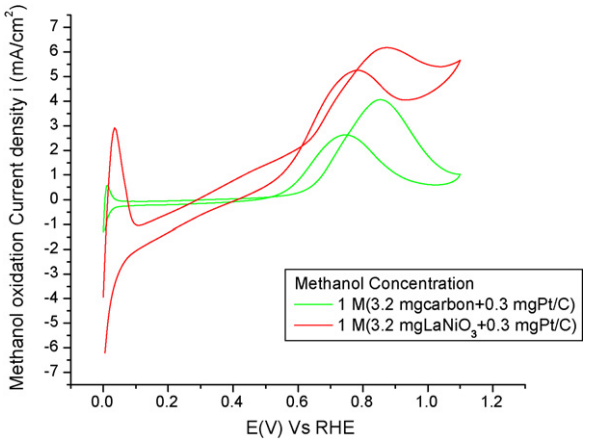

Fig. 9. Cyclic voltammograms for methanol oxidation at 3.2 mg $LaNiO_3$ + 0.3 mg Pt/C and 3.2 mg carbon + 0.3 mg Pt/C coated over glassy carbon electrode in 0.5 M H_2SO_4.

a marginal increase in current (Fig. 6) compared with that of Pt/C where there is a large increase (Fig. 7) during the forward scan for a change in concentration of methanol from 0 to 1 M. This indicates that Pt/C, and not $LaNiO_3$, is a good catalyst for methanol oxidation. However, as we are interested in examining the effect of $LaNiO_3$ on methanol oxidation current, we have compared the specific activity of Pt towards methanol oxidation for $LaNiO_3$ mixed with small amounts of 75% Pt/C (in 3 different ratios) and for carbon mixed with 75%Pt/C (in the same 3 different ratios) with the total weight of the catalyst mixture taken to be 3.5 mg. The results are shown in Figs. 8–10. The onset potential, anodic peak potential and anodic peak current for methanol oxidation for the above three compositions based on $LaNiO_3$ and carbon are given in Table 1 and Table 2, respectively. The anodic peak currents for methanol oxidation for 1 M methanol on $LaNiO_3$-mixed Pt/C are higher than for carbon mixed-Pt/C (Figs. 8–10, Tables 1 and 2). In addition, it can be seen that with increase in the amount of 75% Pt/C added to either $LaNiO_3$ or carbon, there is an increase in the methanol oxidation peak current; the increase is greater for $LaNiO_3$. This suggests that there is a synergistic effect when $LaNiO_3$ is added to Pt/C. White and Sammells [7] in their pioneering work on methanol oxidation on perovskite surfaces have proposed the steps occurring during the oxidation of methanol on perovskite surfaces. They concluded that methanol would initially adsorb on to the perovskite transition metal B-lattice site, while simultaneously losing its alcoholic proton to a basic oxide site. The methoxy species so formed will be oxidatively decomposed by concomitant proton abstraction from

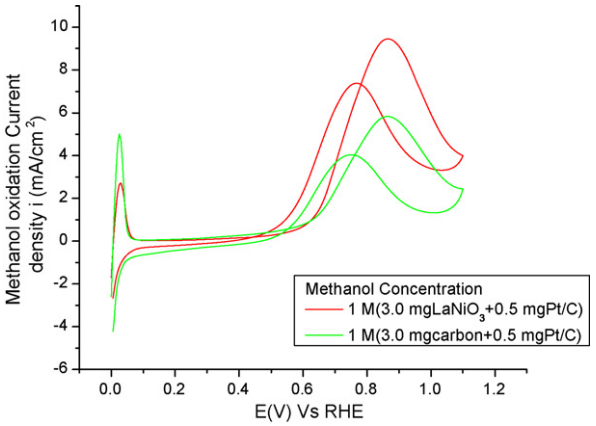

Fig. 10. Cyclic voltammograms for methanol oxidation at 3.0 mg $LaNiO_3$ + 0.5 mg Pt/C and 3.0 mg carbon + 0.5 mg Pt/C coated over glassy carbon electrode in 0.5 M H_2SO_4.

methyl moiety and electron transfer to the reducible metal at the B-lattice site, forming a strongly adsorbed carbon monoxide species. This latter, strongly bound, CO intermediate is expected to become removed from the electrocatalyst surface by reaction with surface oxygen, subsequent electron transfer to the B-site metal, and release of carbon dioxide oxidation product. The resulting oxygen ion vacancy in the perovskite will react with water in the aque-

Table 1
Electrochemical data for $LaNiO_3$, Pt/C and $LaNiO_3$ with Pt/C for methanol oxidation

S. no.	Catalyst composition	Onset of methanol oxidation potential (V vs. RHE)	Anodic peak potential for methanol oxidation in (V vs. RHE)	Anodic peak current for 1 M MeOH (mA)
1	3.5 mg $LaNiO_3$	0.400	–	–
2	3.5 mg Pt/C	0.609	0.995	8.103
3	0.5 mg Pt/C + 3.0 mg $LaNiO_3$	0.625	0.865	0.427
4	0.3 mg Pt/C + 3.2 mg $LaNiO_3$	0.617	0.875	0.279
5	0.1 mg Pt/C + 3.4 mg $LaNiO_3$	0.644	0.860	0.115

Table 2
Electrochemical data for Carbon with Pt/C for methanol oxidation

S. no.	Catalyst composition	Onset of methanol oxidation potential (V vs. RHE)	Anodic peak potential for methanol oxidation in (V vs. RHE)	Anodic peak current for 1 M MeOH (mA)
1	0.5 mg Pt/C + 3.0 mg Carbon	0.633	0.865	0.263
2	0.3 mg Pt/C + 3.2 mg Carbon	0.619	0.855	0.184
3	0.1 mg Pt/C + 3.4 mg Carbon	0.636	0.870	0.081

ous methanol to replace the reacted surface lattice oxygen ion. The increased oxidation current due to the addition of $LaNiO_3$ to Pt/C in the three mixtures containing $LaNiO_3$ may be explained either by the additional catalyst site of the perovskite or by the removal of CO poisoning on the Pt surface by the surface oxygen of the adjacent perovskite, followed by electron transfer to the B-site metal, and release of carbon dioxide oxidation product.

4. Conclusions

Highly crystalline $LaNiO_3$ micro-powders have been successfully synthesized by using a nitrilotriacetic acid precursor route employing $La(NO_3)_3{\cdot}6H_2O$, $Ni(NO_3)_2{\cdot}6H_2O$, NaOH and NTA as starting materials. The decomposition of the precursor complex at 900 °C for 4 h leads to the formation of $LaNiO_3$ powder as confirmed by XRD. The electrical conductivity for $LaNiO_3$ is lower than that prepared by Wang et al. [11] and is $6.125 \times 10^{-2}\,S\,cm^{-1}$ at room temperature. The SEM images and particle-size distribution of the perovskite indicate the formation of micro-powders from the agglomeration of nanoparticles. This catalyst material in conjunction with small amounts of Pt/C at three different ratios has been tested for its catalytic activity towards methanol oxidation. The increased oxidation current due to the addition of $LaNiO_3$ to small amounts of Pt/C in the three mixtures containing $LaNiO_3$ is attributed to either the additional catalytic site of the perovskite in addition to Pt site, or the removal of CO poisoning on the Pt surface by the surface oxygen of the adjacent perovskite.

Acknowledgements

The authors thank the Centre for Education (CFE), the staff of the Central Instrumental Facility for the use of TGA/DTA, SEM, XRD and particle size analyzer, the Department of Science and Technology (DST) (Government of India), for financial support, and the Director of CECRI for institutional support.

References

[1] E. Casado-Rivera, D.J. Volpe, L. Alden, C. Lind, C. Downie, T. Vazquez-Alvarez, A.C.D. Angelo, F.J. DiSalvo, H.D. Abruna, J. Am. Chem. Soc. 126 (2004) 4043.
[2] D.R.M. Godoi, J. Perez, H.M. Villulas, J. Electrochem. Soc. 154 (2007) B474–B479.
[3] H. Wendt, E.V. Spinace, A. Oliveira Neto, M. Linardi, Quim. Nova 28 (2005) 1066–1075.
[4] A. Lan, A.S. Mukasyan, J. Phys. Chem. 111 (2007) 9573–9582.
[5] H. Tamura, H. Yoneyama, Y. Matsumoto, in: S. Trasatti (Ed.), Electrodes of Conductive Metallic Oxides, Part A, Elsevier, Amsterdam, 1981, pp. 262–263.
[6] X. Zhou, B. Hu, Z. Chen, F. Delgado, R. Srivastava, Electrochem. Solid State Lett. 8 (2005) A616–A618.
[7] J.H. White, A.F. Sammells, J. Electrochem. Soc. 140 (1993) 2167–2177.
[8] N. Tien-Thao, H. Alamdari, M.H. Zahedi-Niaki, S. Kaliaguine, Appl. Catal. A: Gen. 311 (2006) 204–212.
[9] F. Gaillard, J.P. Joly, A. Boréave, P. Vernoux, J.-P. Deloume, Appl. Surf. Sci. 253 (2007) 5876–5881.
[10] G. Shabbir, A.H. Qureshi, K. Saeed, Mater. Lett. 60 (2006) 3706–3709.
[11] H. Wang, Y. Zhu, P. Liu, W. Yao, J. Mater. Sci. 38 (2003) 1939–1943.
[12] K. Deshpande, A. Mukasyan, A. Varma, J. Power Sources 158 (2006) 60–68.
[13] M. Ravi kumar, A.K. Shukla, J. Electrochem. Soc. 143 (1996) 2601–2606.
[14] K.W. Andrews, D.J. Dyson, S.R. Keown, Interpretation of Electron Diffraction Patterns, Adam Hilger, London, 1968, pp. 70–80.